

Annual cycles of sea level and sea surface temperature in the western Mediterranean Sea

Catherine Bouzinac¹

European Space Research and Technology Centre, European Space Agency, Noordwijk, Netherlands

Jordi Font

Institut de Ciències del Mar, Consejo Superior de Investigaciones Científicas, Barcelona, Spain

Johnny Johannessen

Nansen Environmental and Remote Sensing Center, Bergen, Norway

Geophysical Institute, University of Bergen, Bergen, Norway

Received 27 February 2002; revised 14 October 2002; accepted 21 October 2002; published 1 March 2003.

[1] In the western Mediterranean Sea, sea level variations are the result of seasonal steric effect, atmospheric forcing and mesoscale circulation activity, particularly in the Alboran and Algerian basins, as well as water mass budget variations including flux variations through the Straits of Gibraltar and Sicily. However, the partition of the magnitude of the sea level variations associated with these different components remains a challenging problem. A better determination of the steric effect component will allow a better knowledge of the other annual components. The aim of this study is to improve the estimation and understanding of the annual sea level variations in the different basins of the western Mediterranean Sea, using sea level anomalies (SLA) derived from TOPEX/POSEIDON and ERS-1/2 altimeters and sea surface temperatures (SST) derived from NOAA/AVHRR infrared imagery, obtained between 1992 and 1998. The first mode of empirical orthogonal function (EOF) analysis on SLA is annual and represents 63% of the total variance. The first mode of EOF analysis on SST anomalies is also annual and represents 98% of the total variance. The lag between the annual variations of SLA and SST is about 40 days. From these EOF results and a parameterisation of the mixed layer, the seasonal dynamic height and the steric effect are estimated and removed from the SLA. The remaining signal is used to examine the annual cycles of the sea level due to water mass budget variations, mesoscale oceanic variability and atmospheric forcing.

INDEX TERMS: 4223 Oceanography: General: Descriptive and regional oceanography; 4275 Oceanography: General: Remote sensing and electromagnetic processes (0689); 4520 Oceanography: Physical: Eddies and mesoscale processes; 4556 Oceanography: Physical: Sea level variations; 4572 Oceanography: Physical: Upper ocean processes; **KEYWORDS:** Mediterranean, sea level, steric effect, seasonal variations

Citation: Bouzinac, C., J. Font, and J. Johannessen, Annual cycles of sea level and sea surface temperature in the western Mediterranean Sea, *J. Geophys. Res.*, 108(C3), 3059, doi:10.1029/2002JC001365, 2003.

1. Introduction

[2] The surface layer of the western Mediterranean Sea is mainly filled by water of Atlantic origin that portrays a cyclonic circulation path. The fresher Atlantic Water (AW) enters the Mediterranean Sea via the Strait of Gibraltar and spreads over the local saltier waters. As it propagates within the surface layer, the AW gradually loses its original properties. It is subject to evaporation and mixing, causing a progressive downstream increase of salinity. After the

anticyclonic gyres in the Alboran basin and the Almeria-Oran jet [Tintore *et al.*, 1988], the AW flows eastward, forming the Algerian Current, along the North African coast until the Channel of Sardinia [Millot, 1985; Font *et al.*, 1998]. Further east, the AW flow divides into two veins (Figure 1), one toward the Tyrrhenian basin and the other toward the Strait of Sicily [Bethoux, 1980]. For a detailed description of the surface circulation in the western Mediterranean Sea, see Millot [1999].

[3] The Algerian Current becomes unstable east of the Greenwich meridian and generates meanders and eddies that can sporadically deviate the AW flow northward. Some of the anticyclonic eddies can become very large and persist for several months in the Algerian basin, while the cyclonic ones disappear rapidly [Millot, 1987; Taupier-Letage and

¹Now at European Space Agency, Noordwijk, Netherlands.

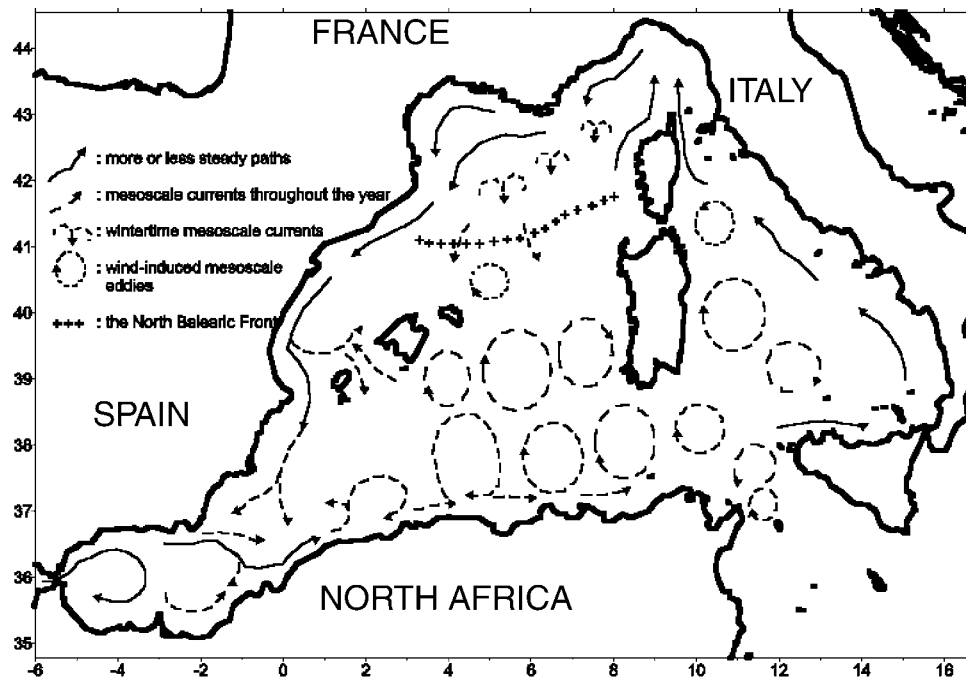


Figure 1. Circulation of the Atlantic Water (AW) in the western Mediterranean Sea, from Millot [1999]. (Reprinted from C. Millot, Circulation in the Western Mediterranean Sea, *Journal of Marine Systems*, 20, 423–442, copyright 1999, with permission from Elsevier Science.)

Millot, 1988]. Benzohra and Millot [1995] have documented one of these anticyclonic eddies, with a diameter of about 130 km, interacting with the entire Algerian Current. In the western part of the Channel of Sardinia, Fuda *et al.* [2000] and Bouzinac *et al.* [1999] have confirmed, from in situ and remote-sensing observations, that anticyclonic eddies strongly interact with the surrounding mean currents, from the surface down to the deep layers. As first described by Millot [1985], the Algerian basin is therefore characterized by a large mesoscale activity in the surface layer acting as a buffer zone between the Atlantic flow entering via the Strait of Gibraltar and the AW flowing eastward via the Channel of Sardinia.

[4] In the northern part of the western Mediterranean Sea, the main feature of the AW circulation is the Northern Current, formed in the Ligurian basin by the junction of the northward currents along each side of Corsica. This main current is defined up to the Catalan basin [Font *et al.*, 1988], following the continental slope of Italy, France and Spain. The mesoscale variability of this current is more intense during fall and winter than during spring and summer, and mainly appears through meanders [Crepon *et al.*, 1982]. The higher flux values in winter seem to be linked to the narrowness and shoreward shift of the current [Alberola *et al.*, 1995] and to the dense water formation occurring in the central zone of the basin. The dense water formation [Gascard, 1978], bounded to the north by the Northern Current, could indeed be the major forcing of the circulation in that region. According to numerical models [Madec *et al.*, 1991], the dense water formation occurring during the winter could force a cyclonic circulation that would persist throughout the year.

[5] Altimetry has become a powerful tool to understand the physics and dynamics of the surface circulation in the

Mediterranean Sea [Ayoub *et al.*, 1998]. At any location, the sea surface height is the sum of various components: geoid, astrophysical tides, mean dynamic topography, atmospheric forcing, steric effect, water mass budget and circulation variations. Annual cycles in sea level can be expected because the primary driving forces of ocean circulation, momentum and surface fluxes, have strong seasonal changes. However, such cycles in sea level are difficult to measure [Zlotnicki *et al.*, 1989]. As first shown by Larnicol *et al.* [1995] with the data from the TOPEX/POSEIDON (T/P) altimetric mission, the annual cycle of the Mediterranean Sea level has an amplitude of about 10 cm. Bouzinac *et al.* [1998] have analyzed the sea level variability in the region of the Algerian Current. Using complex empirical orthogonal functions (EOF), they show that 80% of the total sea level variance (116 cm^2) in the region is due to the annual cycle, while standard deviations of 5 cm are due to high mesoscale activity in some locations of the Algerian basin. More recently, Vignudelli *et al.* [2000] have observed that the steric effect could play a significant role in the seasonal variation of the surface circulation between the Tyrrhenian and Ligurian basins.

[6] Due to small tidal induced sea level variations and the proximity of various laser stations, the western Mediterranean Sea is an attractive site for the altimeter calibration and validation for the Envisat [European Space Agency, 1998, 1999] and Jason [Centre National d'Etudes Spatiales, 2000] altimetric missions. In this context, it is necessary to have a better estimation of the different components that contribute to the sea level variability. The objectives of this study are therefore to analyze the sea level anomalies (SLA) and the sea surface temperatures (SST) using EOF and correlation, and to estimate the steric annual cycle, taking into account both climatological hydrology and SST observations. The

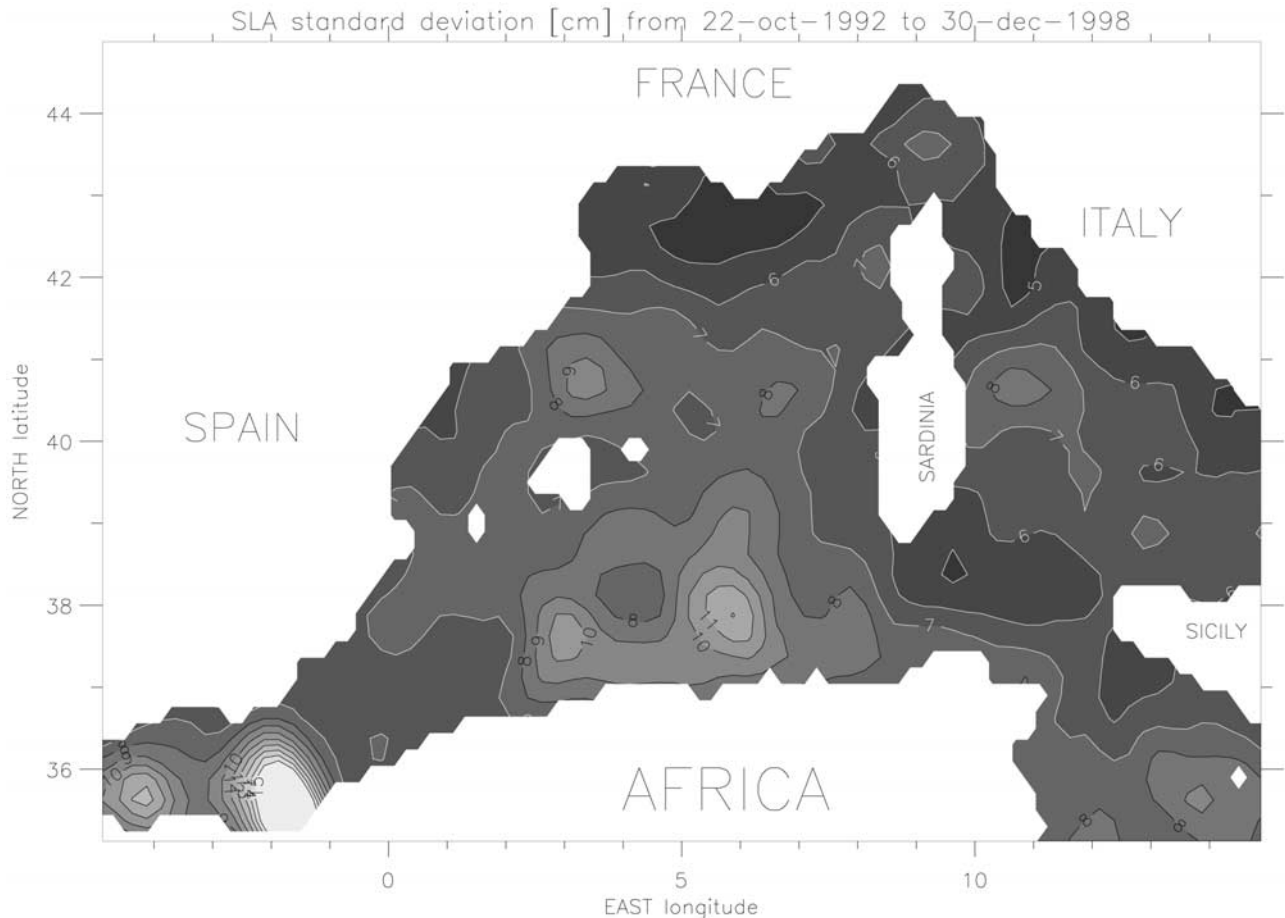


Figure 2. Sea level anomaly (SLA) standard deviation between 22 October 1992 and 30 December 1998 with a contour interval of 1 cm.

interest will be focused on the estimation of the annual steric amplitude in the different basins of the western Mediterranean Sea, followed by an attempt to explain the remaining annual cycle.

[7] The paper is outlined with a short presentation of the data sets in section 2, followed by the EOF and correlation analyses in section 3. In section 4, the computations of the different annual cycles of sea level are detailed and discussed. Section 5 gives the conclusions of this study.

2. Data Sets

2.1. Sea Level Anomaly Maps

[8] The altimetric data set used for this study contains 179 maps of SLA over the western Mediterranean Sea, from 5°W to 15°E in longitude and from 35°N to 45°N in latitude, with a spatial resolution of 0.25° (about 25 km). These SLA maps were obtained from the final process combining T/P, ERS-1 and ERS-2 data, the latter from June 1996 onwards, using an improved space/time objective analysis that takes into account long wavelength error correlated noise [Le Traon et al., 1998]. There is a map every 10 days between 22 October 1992 and 30 December 1998, with a gap between 6 December 1993 and 10 April 1995, due to the geodetic mission of ERS-1. This data set has been produced and provided by AVISO-CLS as part of the Environment and Climate EU AGORA (ENV4-

CT9560113) and DUACS (ENV44-T96-0357) projects. SLA are relative to a 3-year mean (1993–1995). A specific process was performed to obtain an ERS-1/2 mean consistent with the T/P mean. T/P MGDR (version C) reprocessed by AVISO were used [AVISO, 1996]. Atmospheric pressure from the European Centre for Medium-range Weather Forecast (ECMWF) was used to apply the inverse barometer correction. This version includes, in particular, the JGM3 orbits, the CSR3.0 tidal model and the correction of TOPEX drift. ERS-1/2 data are the OPR distributed by Centre ERS d'Archivage et de Traitement [1996]. Altimetric corrections were updated to be homogenous with T/P and a global adjustment using T/P as a reference was performed to correct for ERS-1/2 orbit error. Additional information is given by Le Traon and Ogor [1998].

[9] The map of standard deviation from the complete SLA data set is shown in Figure 2. The highest sea level variability is found in the Alboran and Algerian basins, with more than 10 cm RMS, due to the mesoscale activity. In the calmer areas, the minimum variability is still 5 cm RMS due to the annual sea level variation [Larnicol et al., 1995; Bouzinac et al., 1998].

2.2. Sea Surface Temperature Maps

[10] The infrared data set used for this study contains 2557 maps of nighttime SST over the western Mediterranean Sea, with a spatial resolution of about 18 km. Daytime

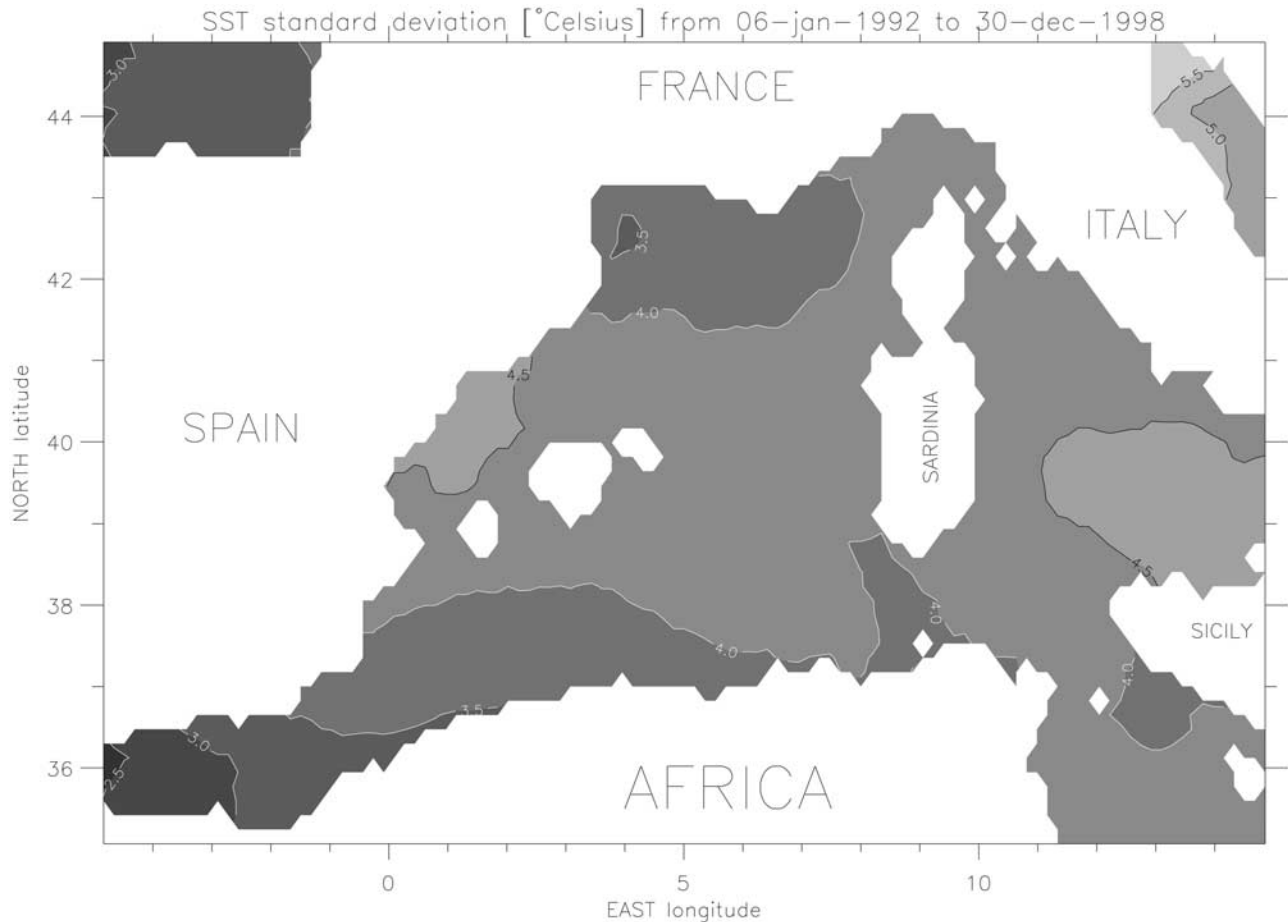


Figure 3. Sea surface temperature (SST) standard deviation between 06 January 1992 and 30 December 1998 with a contour interval of $0.5^{\circ}\text{Celsius}$.

SST have not been used to avoid sunlight-induced warming of the sea surface and to stay as close as possible to the bulk temperature of the mixed layer. There is a map for every night from January 1992 to December 1998. This data set has been produced and provided by PODAAC-JPL, within the frame of the PATHFINDER project [Vazquez *et al.*, 1998]. To collocate these data in time with the SLA maps, the SST maps have been averaged every 10 days, to obtain a time series of 256 SST maps (from 6 January 1992 to 30 December 1998). This also permitted the gaps caused by cloud cover to be filled.

[11] The map of standard deviation from the 256 night SST maps is shown in Figure 3. The variability is about 4°C RMS in the western Mediterranean Sea, but it reduces toward the Strait of Gibraltar due to the smaller annual temperature variation for the Atlantic origin water than for the Mediterranean surface water [Taupier-Letage and Millot, 1988].

2.3. Hydrological Climatology

[12] The hydrology from the Mediterranean Oceanic Database (MODB) [Brasseur, 1995] has been used to compute the surface dynamic heights. This data set (temperature and salinity at depths of 0, 5, 15, 30, 50, 80, 120, 160, 200 m, etc.) is seasonal with a spatial resolution of 0.25° . It has been interpolated, linearly in space and with a cubic convolution in time, to fit the SLA maps. The dynamic

heights relative to the depth of 200 m have been calculated with the UNESCO equations of state for seawater [Millero and Poisson, 1981; Fofonoff and Millard, 1983].

3. EOF Analyses and Correlation

[13] The decomposition into EOF is built on modes calculated from the data themselves, hence proper to the data set and not imposed. Their principal virtue is that they reduce the amount of data by keeping only the most significant phenomena. Real EOF have been preferred to complex EOF for this study due to the more standing than propagating wave aspect of the annual signal. The EOF are computed with the singular value decomposition method [Press *et al.*, 1992]. For each analysis, only the EOF representing a large percentage of the total variance or having an annual periodicity are considered, the total variance being the sum of both the temporal and spatial variabilities.

3.1. EOF Analysis on SLA

[14] The first EOF (EOF1) of the SLA represents 62.8% of the total variance, which is 56.2 cm^2 , while the second and third EOF (EOF2 and EOF3) represent only 4.8% and 3.0%, respectively. The temporal amplitudes of EOF1, EOF2 and EOF3 display a clear annual periodicity. For EOF1, the maximum temporal amplitude is reached in fall

(between October and December) while the minimum is reached in winter (February–March) (Figure 4a). The spatial amplitude of EOF1 (Figure 4b) is positive everywhere due to phase homogeneity, with maximum values in the Alboran and Algerian basins and minimum values in the Provençal basin, between Corsica and Italy and southwest of Sardinia. The temporal amplitude of EOF2 is maximum during the short time of the EOF1 fast decrease (January) (Figure 5a), except for the period 1992–1993 where the general sea level behavior is rather different compared to the period 1995–1998. The spatial amplitude of EOF2 (Figure 5b) shows peak values (positive or negative) mainly in the Algerian basin, the Channel of Sardinia and the Strait of Sicily. The temporal amplitude of EOF3 (Figure 6a) is typically maximum during spring or summer. Its spatial amplitude (Figure 6b) shows that EOF3 is associated with the variability of the western gyre of the Alboran basin and some eddies of the Algerian basin.

[15] This EOF analysis suggests that the steric effect is the main signal captured by EOF1 while other annual components with mesoscale effects seem to be partitioned between the three modes. Some local maximum amplitudes suggest that the rather homogeneous annual cycle contained in EOF1 is apparently disturbed by an annual variation of the circulation. This could be due to the annual AW inflow variation having a great impact on the mesoscale activity which is known to be strong in the Alboran and Algerian basins [Vazquez *et al.*, 1996; Bouzinac *et al.*, 1998]. EOF2 and EOF3 apparently describe the heterogeneous parts of this annual variability with lows and highs in different areas. However, some of the EOF2 and EOF3 features could be intense transient events, which are not statistically significant. Some eddies which can last for several months or a year in the Alboran and Algerian basins could be present in the 3-year mean sea level used to compute the SLA. Therefore, it must be kept in mind that the presence of unreal persistent local anomalies could be due to the use of that short time average.

3.2. EOF Analysis on SST

[16] SST anomaly maps have been created by removing the 7-year mean SST at each grid point. EOF1 of the SST anomalies represents 97.7% of the total variance, which is of 17.0°C^2 . EOF1 shows that almost all the SST variability is due to the seasonal cooling and warming, with minima in February–March and maxima in August–September (Figure 7a). The minimum negative anomaly is smaller in absolute value but longer in duration than the maximum positive anomaly. The maximum amplitudes are obtained in the Catalan and Tyrrhenian basins and minimum amplitudes in the Gulf of Lion and the Alboran basin (Figure 7b). This is confirmed by fitting the function $A\cos(\omega t - \varphi) + C$ to the SST time series (Figure 8) in which ω was set to 2π per year. The map of Figure 8a gives the amplitudes A in $^{\circ}\text{C}$, which are in agreement with the EOF1 spatial amplitudes. The minimum amplitude is observed in the Alboran basin with only 4°C due to the smaller AW temperature variation, while the maximum is observed in the Catalan and Tyrrhenian basins with 6°C . The spatial distribution of the phase φ (Figure 8b) is difficult to interpret but suggests some cycle anomalies due to the Alboran gyres and wind effects around Corsica. The map of the constant C (Figure

8c) corresponds to the 7-year mean SST removed to obtain the SST anomalies.

[17] EOF2 and EOF3 represent only 0.6% and 0.5% of the total variance, respectively. However, the signals are not noisy. Their temporal amplitudes (Figures 9a and 10a) display an annual periodicity. Looking especially at the negative temporal amplitudes of years 1992 and 1993, they seem almost in phase quadrature to each other, EOF2 leading EOF3 by 2 or 3 months. The spatial EOF2 amplitude distribution (Figure 9b) is very similar to the spatial distribution of the phase shown in Figure 8b and is complementary to the spatial EOF3 amplitude distribution (Figure 10b). The latter presents an east-west gradient while the former presents a south-north gradient. Indeed, the combination of these two EOF gives a cyclonic propagating anomaly up to 1°C around the western Mediterranean Sea. The cyclonic propagation of these anomalies could be due to the association of the early cooling from the north and the mean cyclonic circulation of the AW with weaker annual temperature variation than the Mediterranean surface water. Irregular jumps in the time series of EOF2+EOF3 suggest that this mode might be very sensitive to atmospheric conditions.

3.3. Correlation Between SLA and SST

[18] The SST maps have been interpolated on the SLA grid (from a nominal resolution of 18 km to an exact resolution of 0.25°). The correlation coefficient increases with distance away from the main coastal currents and mesoscale activity (Figure 11a) and its spatial distribution is in good agreement with the EOF1 amplitudes from SLA (Figure 4b). This means that in general the highest correlation (between 0.5 and 0.7) is found in regions where the steric signal is large and less perturbed by mesoscale variability. On the other hand, in the Alboran basin where the steric effect is not expected to be large, both the correlation (>0.5) and the SLA variability (>10 cm RMS) are high on the gyres. As mentioned previously, this could be due to the annual water inflow variation through the Strait of Gibraltar and the subsequent evolution of the anticyclonic gyres.

[19] The time lag corresponding to the best cross-correlation is mapped in Figure 11b. It is very variable, however most of the low time lags are associated with high correlation coefficients. A 3D histogram of the correlation versus time lag (Figure 12) shows that a correlation coefficient greater than 0.5 is generally associated with a time lag between 20 and 50 days. Moreover, the cross-correlation between the time series of EOF1 on SLA and EOF1 on SST anomaly is maximum (0.8) for a time lag of 40 days. This suggests that the water column requires a mean time of about 40 days to fully adjust to a surface temperature variation.

4. Annual Cycles of Sea Level Anomaly

4.1. Dynamic Height and Steric Effect Components

[20] Assuming that the night SST is a good estimator of the mixed layer temperature [Robinson, 1985], the amplitude of the steric effect can be derived using the EOF1 of SST and the MODB climatological hydrology at each grid point. This has been achieved by computing the dynamic

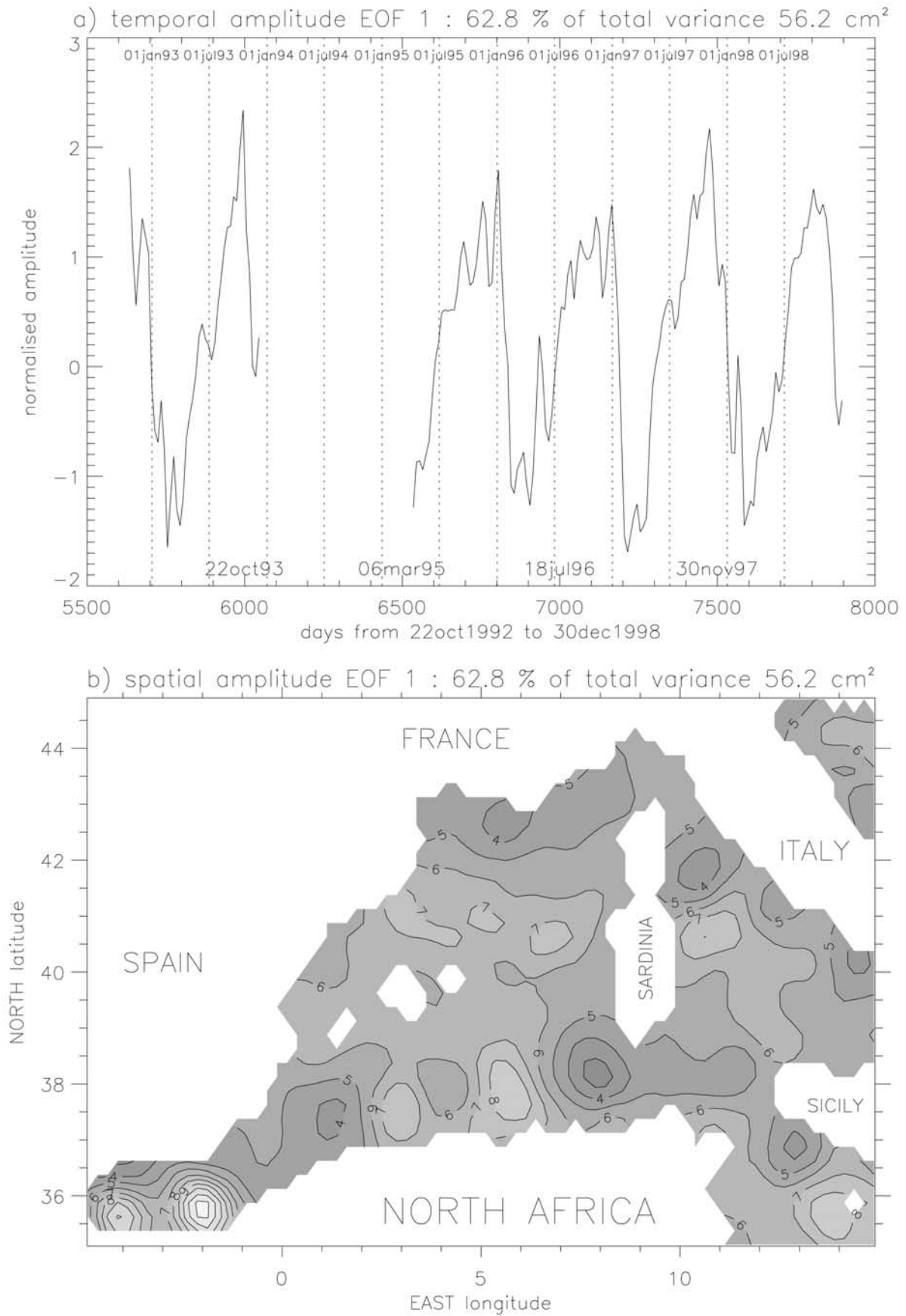


Figure 4. (a) Temporal normalized amplitude and (b) spatial amplitude with a contour interval of 1 cm for EOF 1 from SLA.

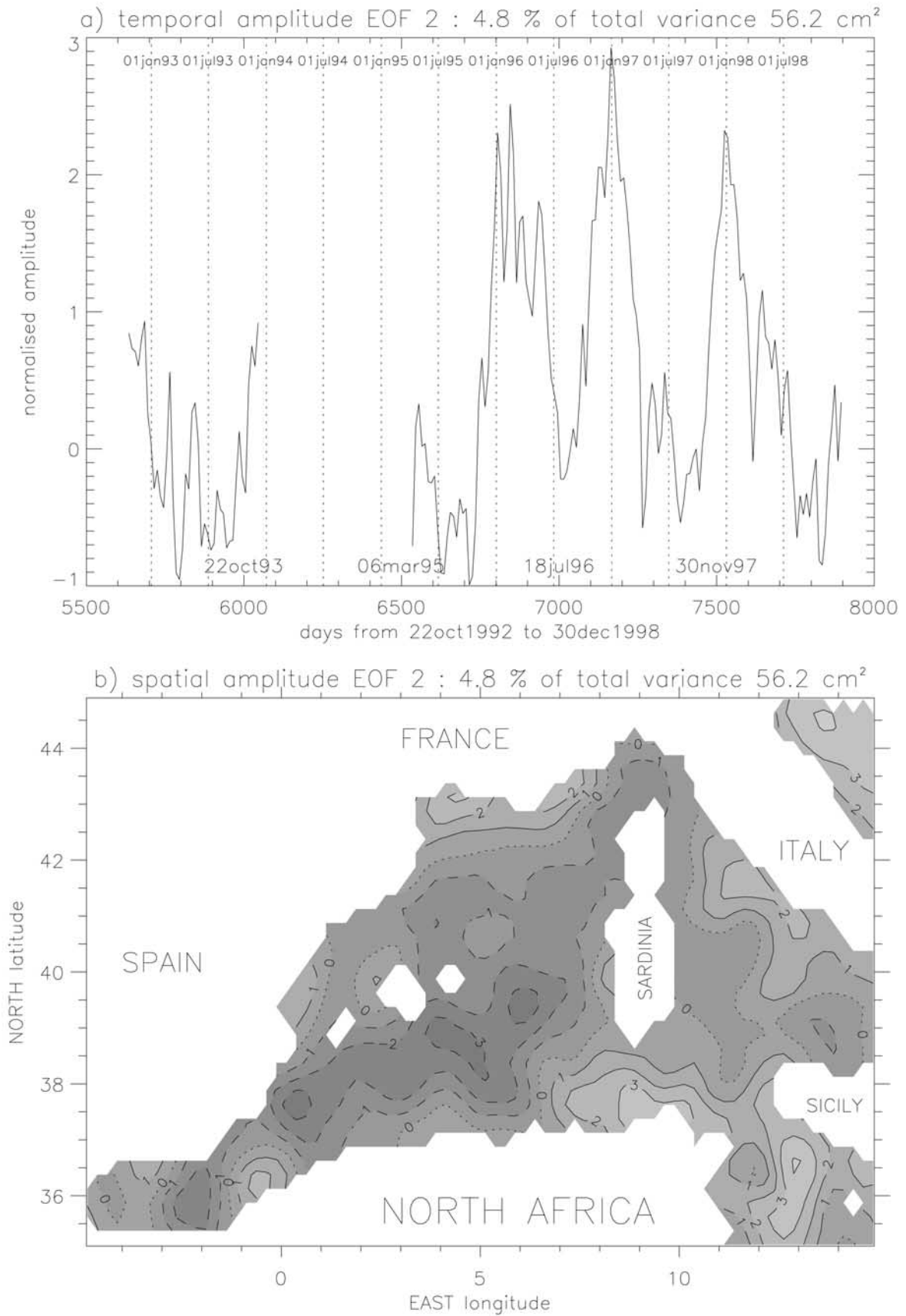


Figure 5. (a) Temporal normalized amplitude and (b) spatial amplitude with a contour interval of 1 cm for EOF 2 from SLA. Dashed, dotted and solid lines correspond to negative, null and positive values, respectively.

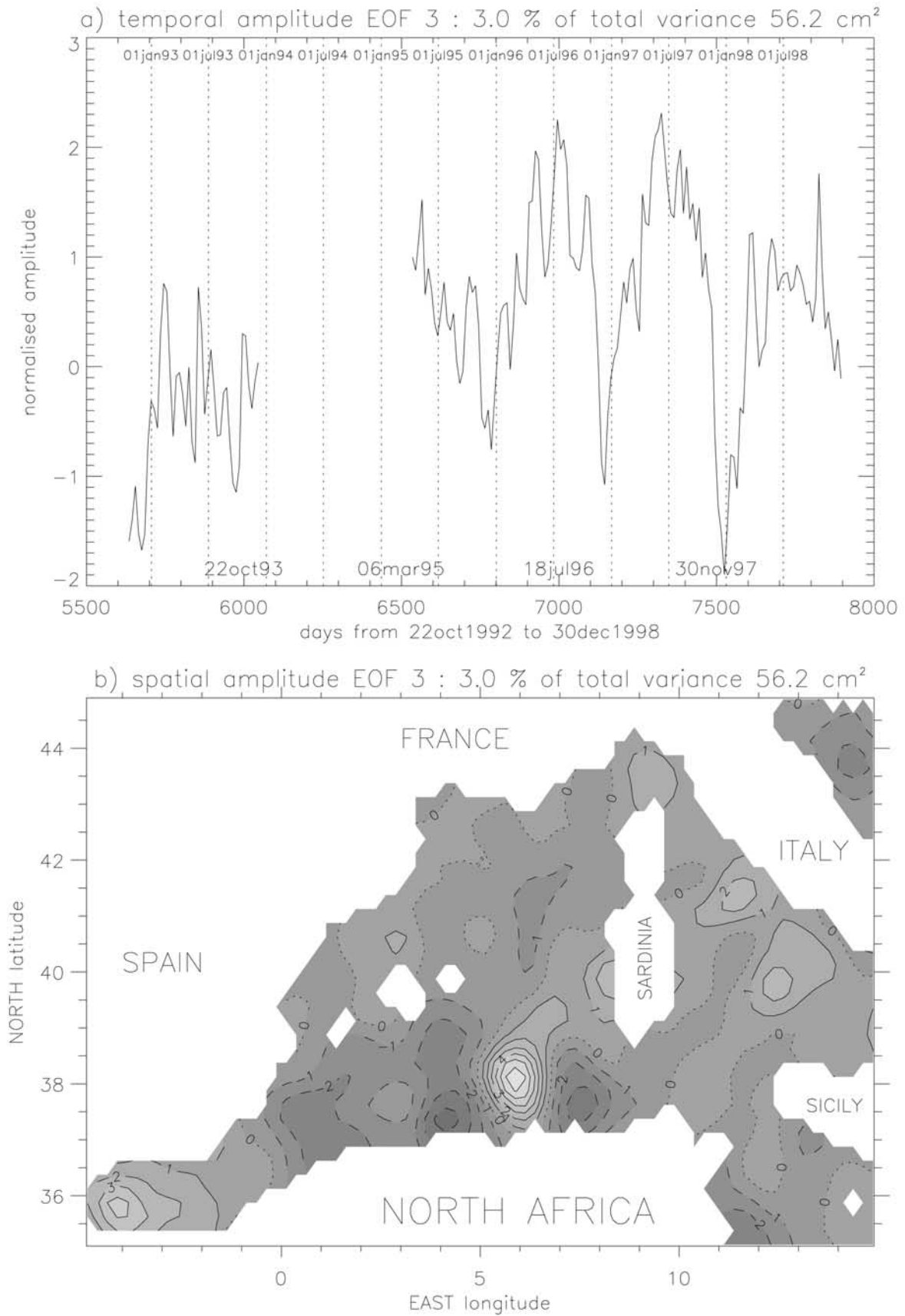


Figure 6. (a) Temporal normalized amplitude and (b) spatial amplitude with a contour interval of 1 cm for EOF 3 from SLA. Dashed, dotted and solid lines correspond to negative, null and positive values, respectively.

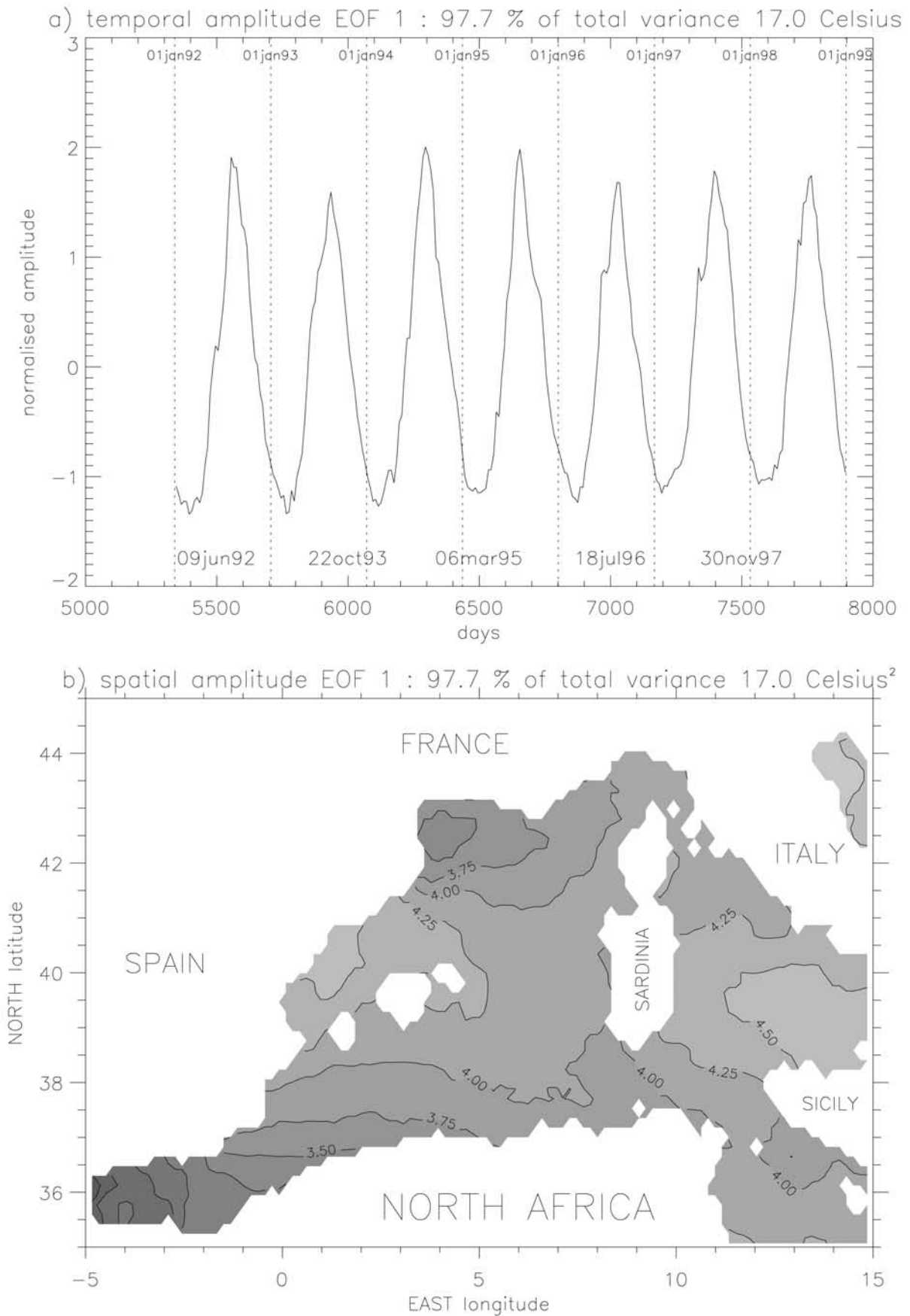


Figure 7. (a) Temporal normalized amplitude and (b) spatial amplitude with a contour interval of $0.25^{\circ}\text{Celsius}$ for EOF 1 from SST anomaly.

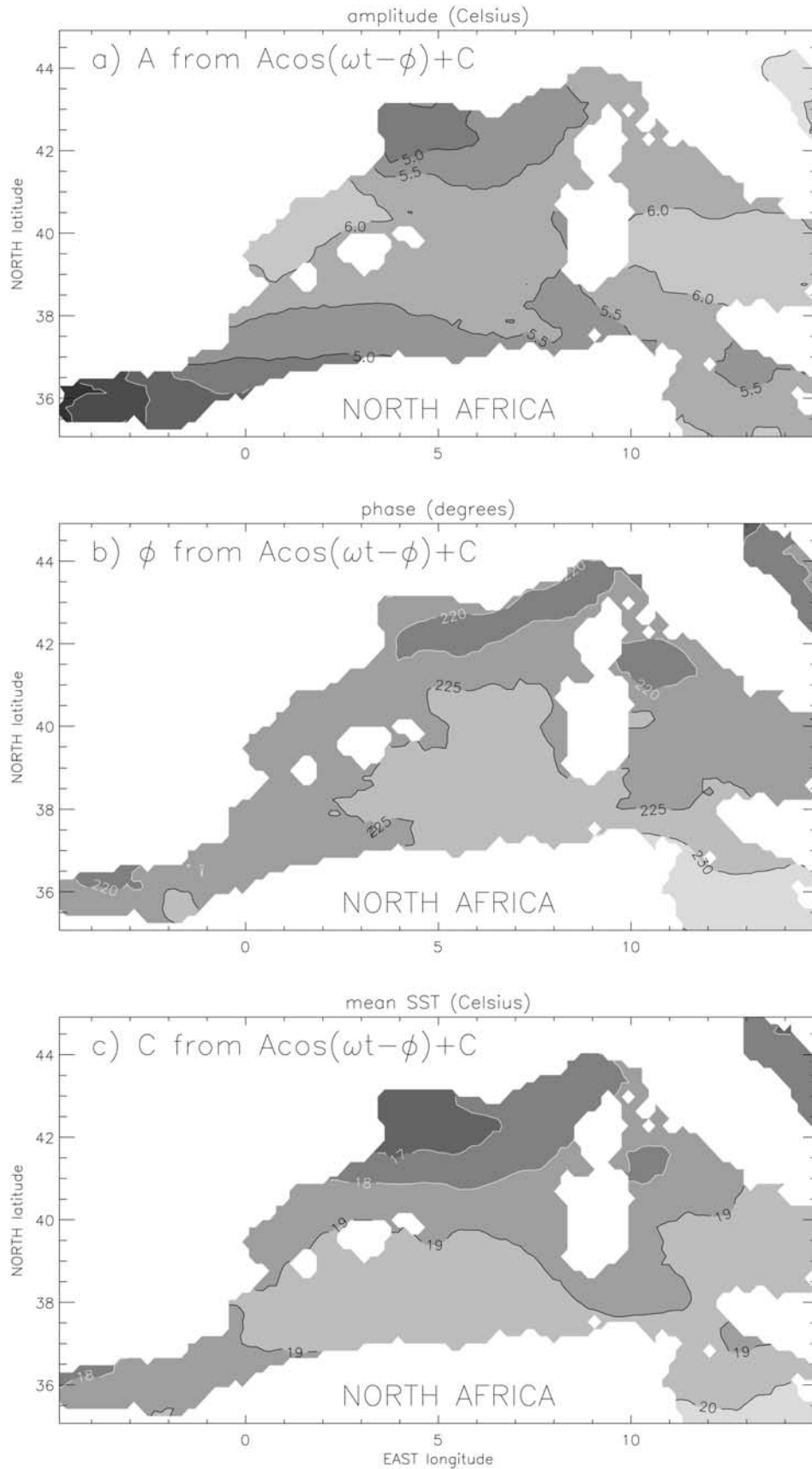


Figure 8. SST fitting to an annual cosine function $A \cos(\omega t + \phi) + C$ where A is the amplitude in Celsius, ϕ is the phase in degrees and C is the average in Celsius.

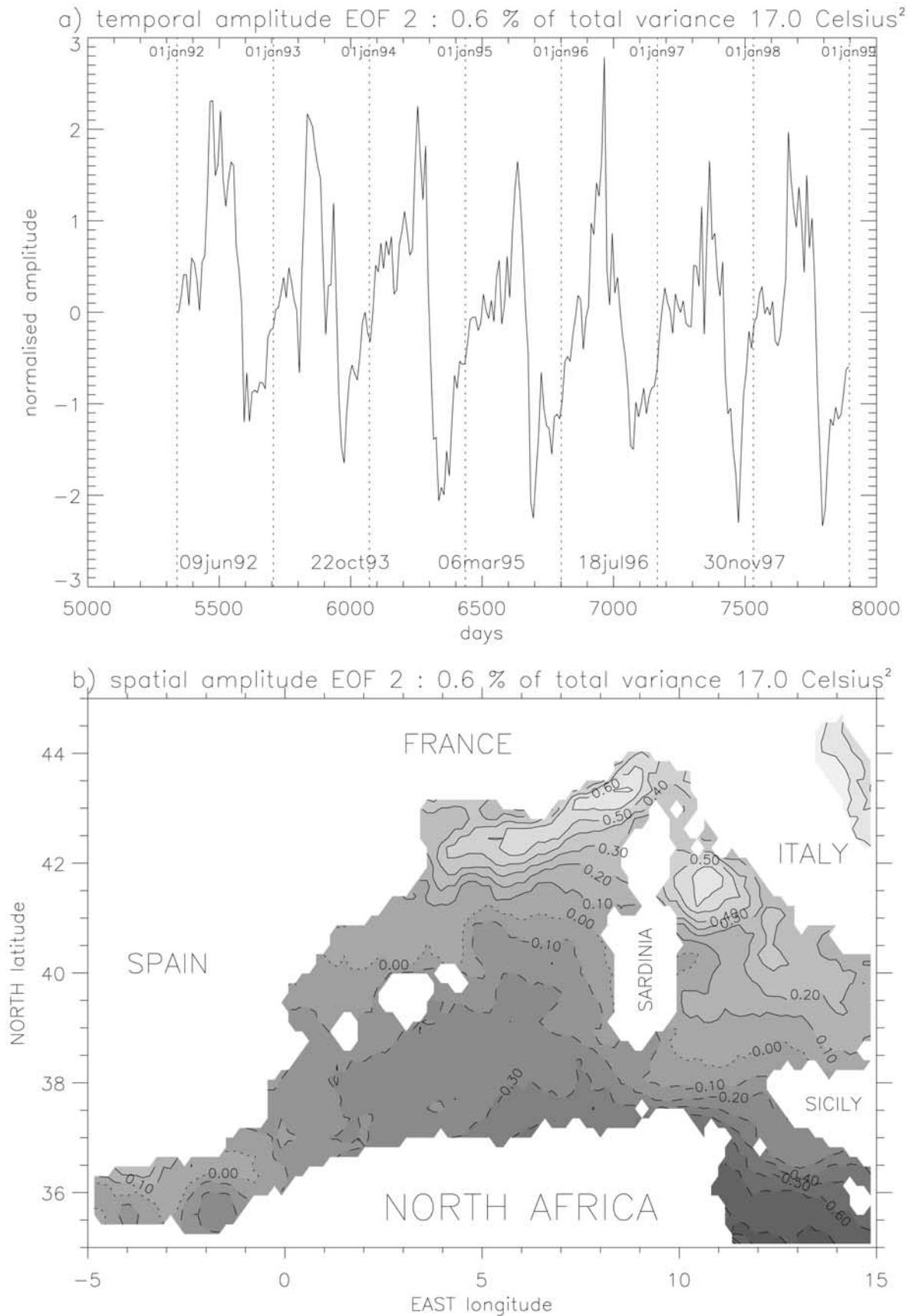


Figure 9. (a) Temporal normalized amplitude and (b) spatial amplitude with a contour interval of 0.1°Celsius for EOF 2 from SST anomaly. Dashed, dotted and solid lines correspond to negative, null and positive values, respectively.

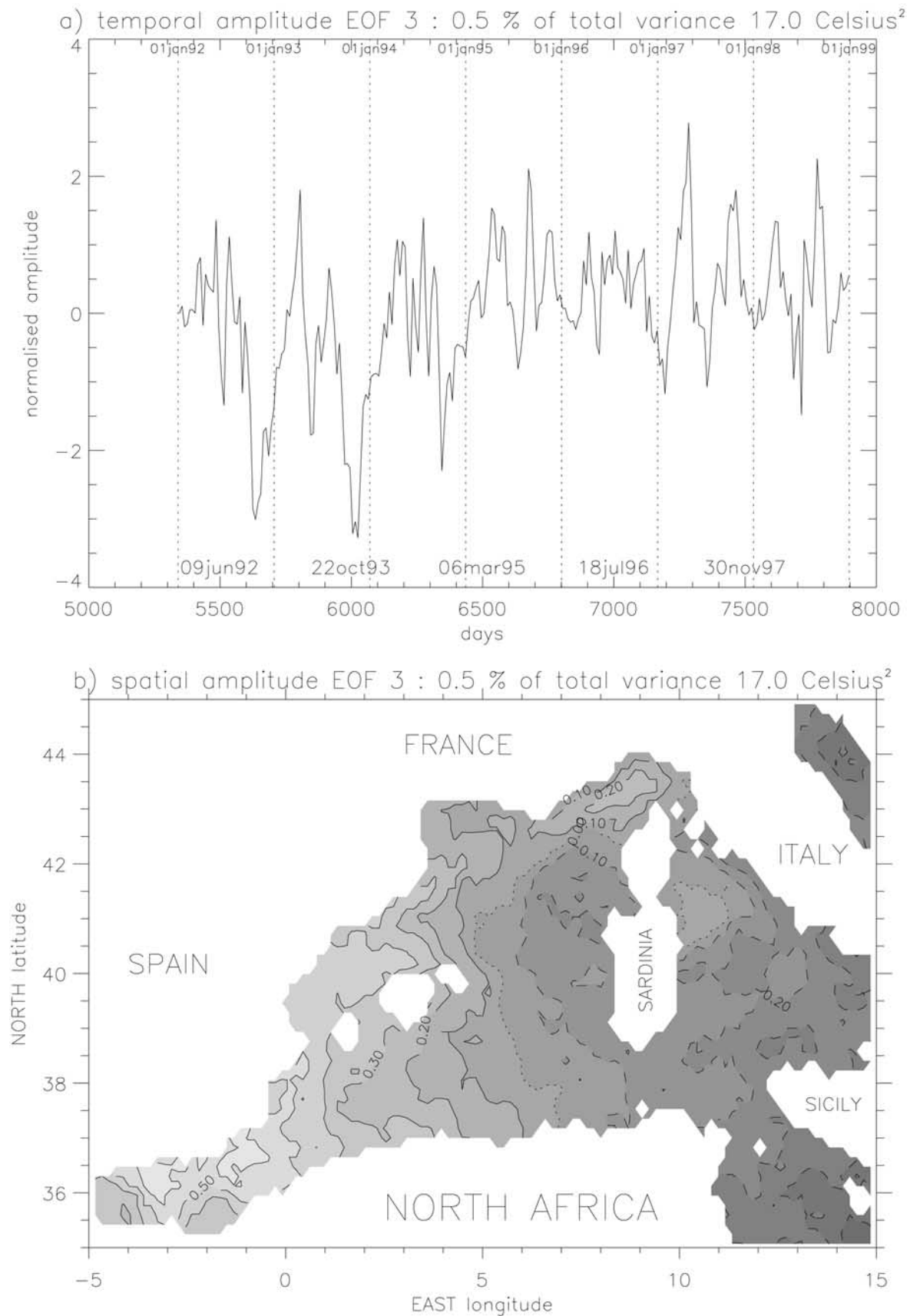


Figure 10. (a) Temporal normalized amplitude and (b) spatial amplitude with a contour interval of $0.1^{\circ}\text{Celsius}$ for EOF 3 from SST anomaly. Dashed, dotted and solid lines correspond to negative, null and positive values, respectively.

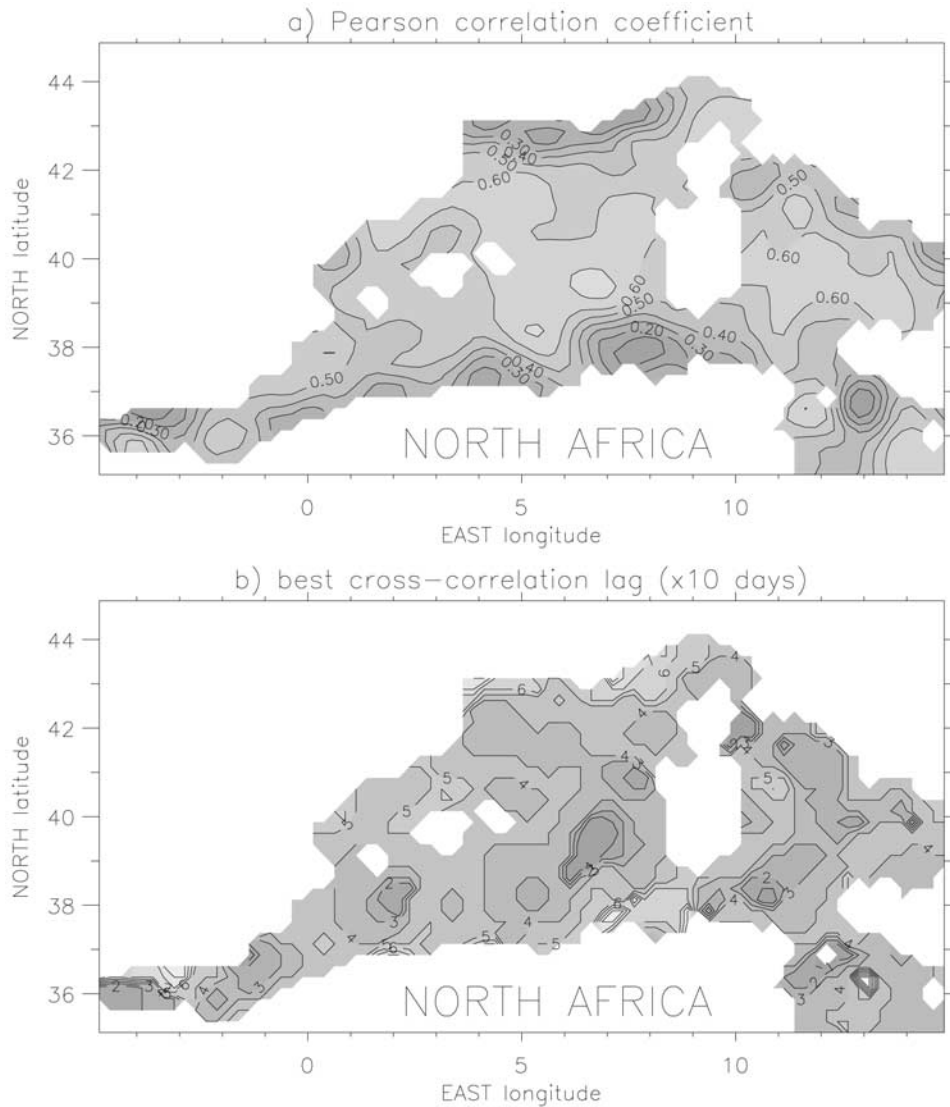


Figure 11. (a) Correlation between SLA and SST time series with a contour interval of 0.1. (b) Lag of the best cross-correlation between SLA and SST time series with a contour interval of 10 days.

height anomaly of the surface layer, using SST EOF1 temperatures in the mixed layer and climatological MODB temperatures below. The climatological MODB salinities have been used at all depths. These anomalies are relative to the 7-year mean dynamic height and are therefore the result of the steric effect and the annual geostrophic surface circulation variations. They are called steric+dynamic anomalies (SDA) in the following text.

[21] The choice of the reference depth of 200 m is a compromise to account for hydrology well below the mixed layer and to allow for estimation as close as possible to the coasts. The same computation has been performed with a reference depth of 500 m. The standard deviation of the difference between both resulting SDA sets is 0.4 cm. Therefore, it appears that the role of the 200- to 500-m layer has a small impact on the annual sea level variation which can be neglected considering the centimeter order of magnitude.

[22] The thickness of the mixed layer (depth of the thermocline) in the western Mediterranean Sea derived from

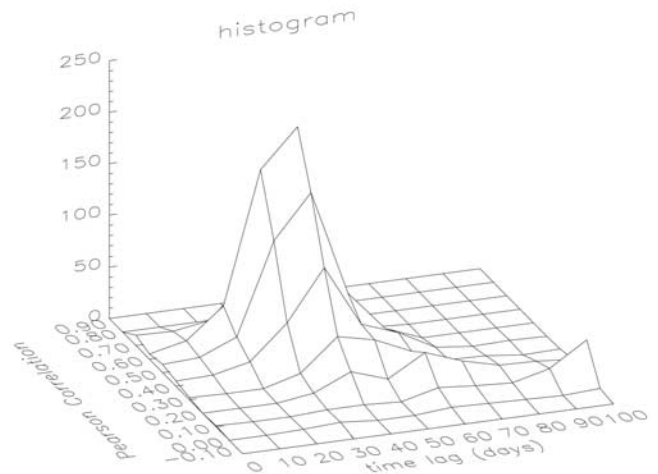


Figure 12. Histogram of the correlation between SLA and SST time series versus the cross-correlation time lag, from the maps shown in Figure 11.

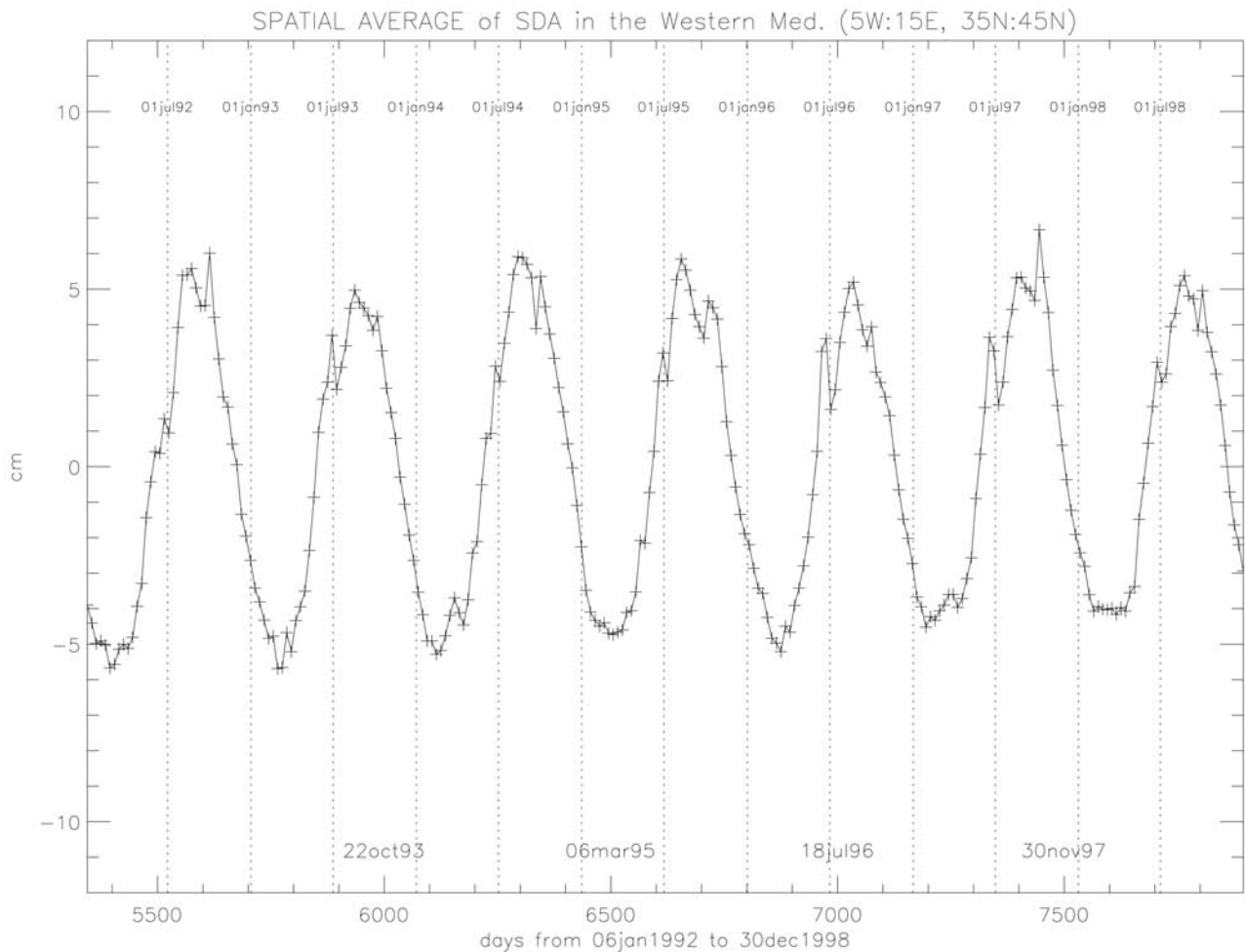


Figure 13. Time series of the steric + dynamic anomaly (SDA) spatial average.

the National Oceanographic Data Center hydrographic (NODC) profiles varies between 10 and 70 m. In order to examine the influence of the choice of the thermocline depth, the same computation has been performed with thicknesses of 30 m and 50 m. The standard deviation of the difference between both SDA sets is 1 cm. Therefore the choice of the thermocline depth has a significant impact on the results. Furthermore, as the mixed layer thickness undergoes significant temporal and spatial variations, the choice of a constant thickness is too simple and not realistic. However, the spatial variations of the thermocline depth in the Mediterranean Sea are even less known than the temporal variations.

[23] Different spatially constant thicknesses of mixed layer have therefore been tried. The choice is limited to the MODB levels. If one assumes that the SDA variations are completely captured by the first EOF on SLA because of the large dominance of the steric effect on the geostrophic variations in the SDA, then a way of checking the quality of the SDA calculation is to obtain the same EOF 2 and 3 from the analysis on SLA and from the analysis on SLA minus SDA (SLA-SDA). Finally, the best choice inferred from the EOF analyses and the NODC and MODB profiles examination is a seasonal variable thickness of 15 m in summer, 50 m in winter and 30 m in spring and fall. The resulting

spatial mean SDA amplitude is 5.2 cm (Figure 13) with positive maximum in August–September and negative maximum in February–March. This mean amplitude is in good agreement with the 5–6 cm obtained by *Cazenave et al.* [1998] with a vertical integration of *Levitus et al.* [1994] climatology from the 1000-m depth to the surface.

[24] Figure 14 shows the map of the amplitude calculated from a cosine function fitting the SDA annual cycle between 1992 and 1998. The largest values (>6 cm) are found in the Catalan and Tyrrhenian basins where the amplitude of the SST annual variation is maximum (Figure 8a) and where the occurrence of AW is rare. The large value (>6 cm) between Ibiza and Spain could be due to surface water trapped in an anticyclonic eddy, warmed up by high SST, during all summer, which disappears during fall as observed by *Bouzinac* [1997] from altimetric SLA of 1993. This scenario is also in agreement with the surface circulation scheme of *Pinot and Ganachaud* [1999]. The smallest SDA amplitudes (<3 cm) are found in the Channel of Sardinia and the Strait of Sicily. The weakest steric signal can be explained by the frequent presence of AW, which regularly spreads over the Channel and the Strait as meanders and eddies. Surprisingly, large SDA (between 5 and 6 cm) are obtained in the western Alboran basin where the gyre variability is important. This could be due to an

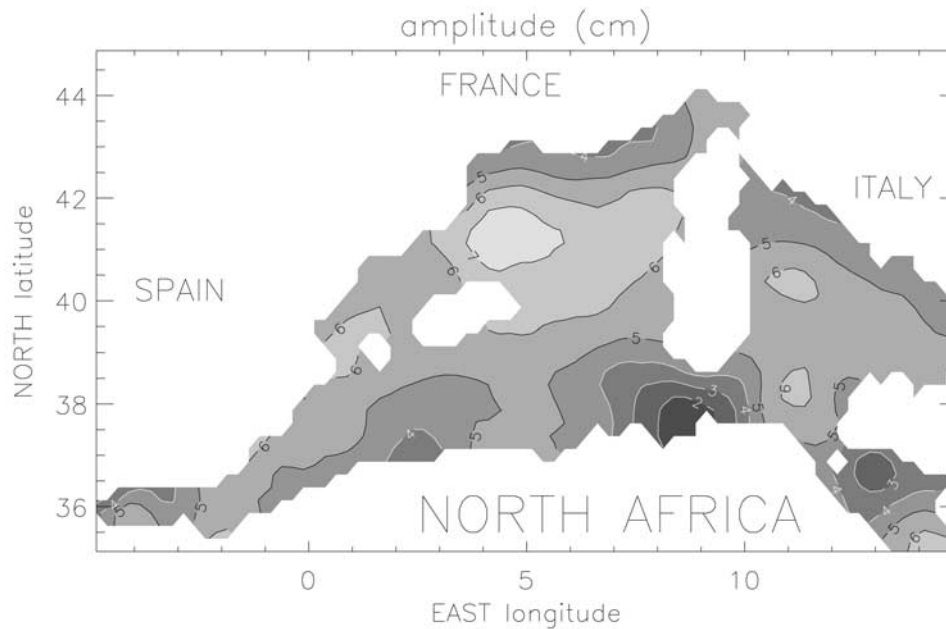


Figure 14. Amplitude of a cosine function fitting to the SDA annual cycle with a contour interval of 1 cm.

overestimation of the mixed layer thickness in that area, to poor quality of the MODB climatology for winter compared to summer, or to the annual variability of the geostrophic surface circulation. Indeed, a numerical modeling study of the Alboran basin [Werner *et al.*, 1988] indicates that the gyres may collapse under the influence of winds and inflow/outflow variations through the Strait of Gibraltar. Hence, a large annual geostrophic variability obtained in the western gyre might be a seasonal response to these two forcing mechanisms [Harzallah *et al.*, 1993].

4.2. Other Annual Components

[25] The SDA has been removed from the SLA with a time lag of 40 days (as obtained from the cross-correlation analysis in section 3.3) at each grid point. An EOF analysis is then performed on the remaining SLA signals (SLA-SDA maps) and the total variance is now 35.1 cm^2 . The first EOF represents 38.0% of the total variance and its main periodicity is still annual (Figure 15a), but it also displays a secondary periodicity of about 6 months already observed by Bouzinac *et al.* [1998] and Garcia and Vazquez [1999]. The spatial amplitude is still positive everywhere, with a background amplitude between 2 and 4 cm, and it is larger in the Alboran basin and along the Algerian and Tunisian coasts (Figure 15b). The second EOF represents 7.8% of the total variance and, as expected, is similar to the EOF2 on SLA (Figures 16a and 16b). The third EOF (Figures 17a and 17b), with 5.2%, remains almost identical to the EOF3 on SLA, except in the Alboran basin where the highest amplitude has shifted from the western gyre to the eastern gyre. This supports the assumption that the SDA estimation is not reliable in the Alboran basin.

[26] Now that the combined annual dynamic and steric components have been roughly eliminated, the first three EOF with annual periodicity represent the remaining annual sea level variations. Even without the SDA component, the

annual cycle of the sea level variation still represents about 50% of the variability, corresponding to a variance of 17.5 cm^2 .

[27] The spatial homogeneity of the first EOF (positive amplitudes everywhere in Figure 15b) with a mean variability of about 3.5 cm suggests that this mode contains mainly the water mass budget variation [Harzallah *et al.*, 1993]. A recent estimation of the climatological monthly mean values for the fresh water budget (evaporation minus precipitation and rivers run-off, E-P-R) gives an annual amplitude of 2.5 cm [Boukthir and Barnier, 1998]. Unfortunately, the compensation of this budget variation by the AW inflow variation is still difficult to determine [Larnicol *et al.*, 1995] due to a poor knowledge of the temporal flux variations at the Straits of Gibraltar and Sicily. However, the remaining amplitude of about 1 cm suggests that the steric signal might not have been completely removed from the SLA in some areas where the mixed layer thickness is underestimated or where the intermediate layer has a significant role in the steric amplitude. Although the inverse barometer correction used for the altimetric SLA is valid for time periods larger than 30 days [Le Traon and Gauzelin, 1997] and therefore for seasonal timescale, signal due to the bad correction of atmospheric pressure quick changes (less than 30 days) might be present in this mode and account for some sharp variations of the temporal amplitude (Figure 15a).

[28] The remaining annual variability is mainly located in the two basins where the mesoscale activity is known to be important and it is shared between the first three EOF. This suggests that this annual signal is due to AW inflow variability, not fully caught by the MODB seasonal climatology, or due to wind-forcing, influencing the mesoscale activity. In a study of the 1992-1993 period, Garcia and Vazquez [1999] have found a significant correlation between sea level and wind stress curl annual variability in the

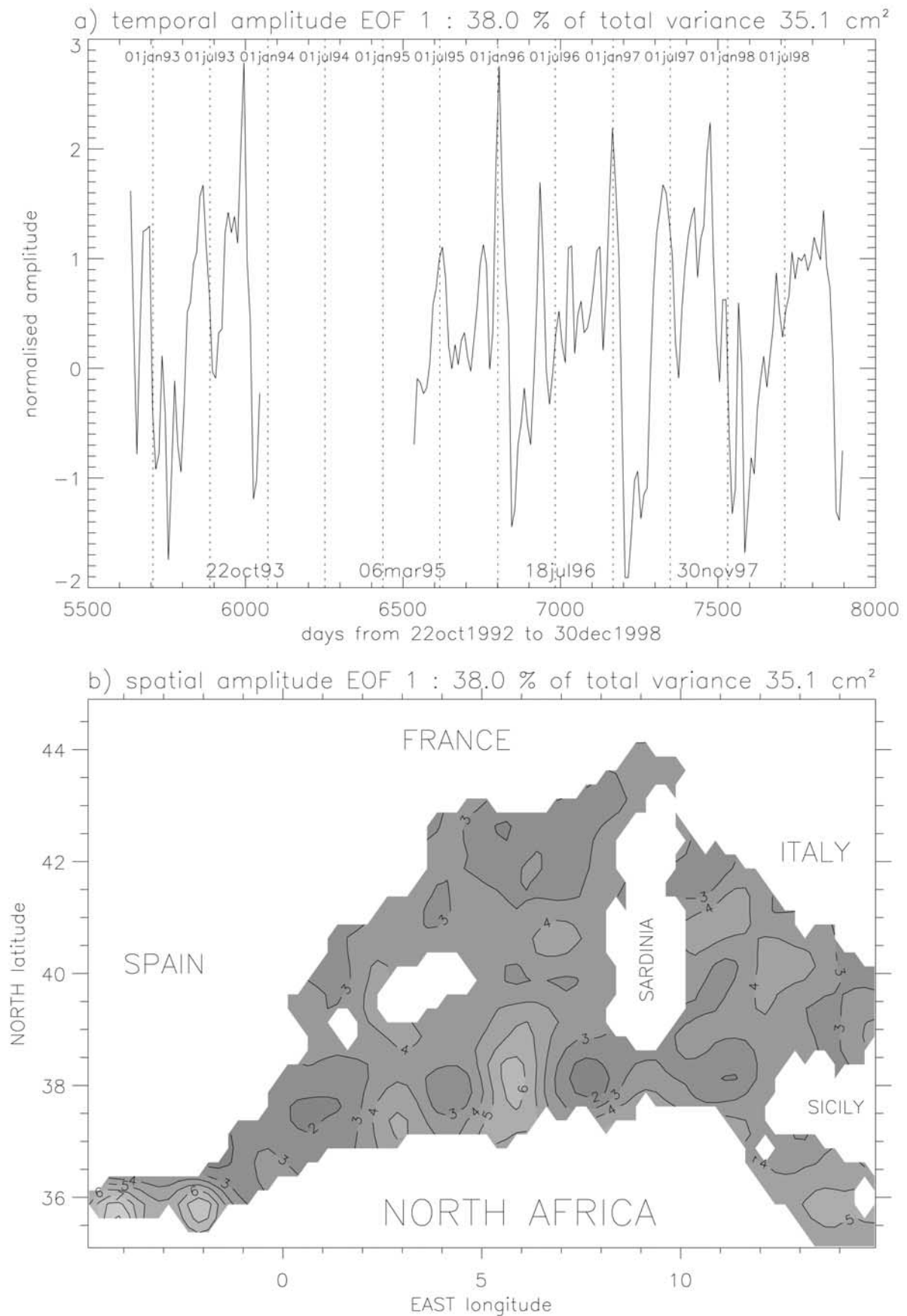


Figure 15. (a) Temporal normalized amplitude and (b) spatial amplitude with a contour interval of 1 cm for EOF 1 from SLA-SDA.

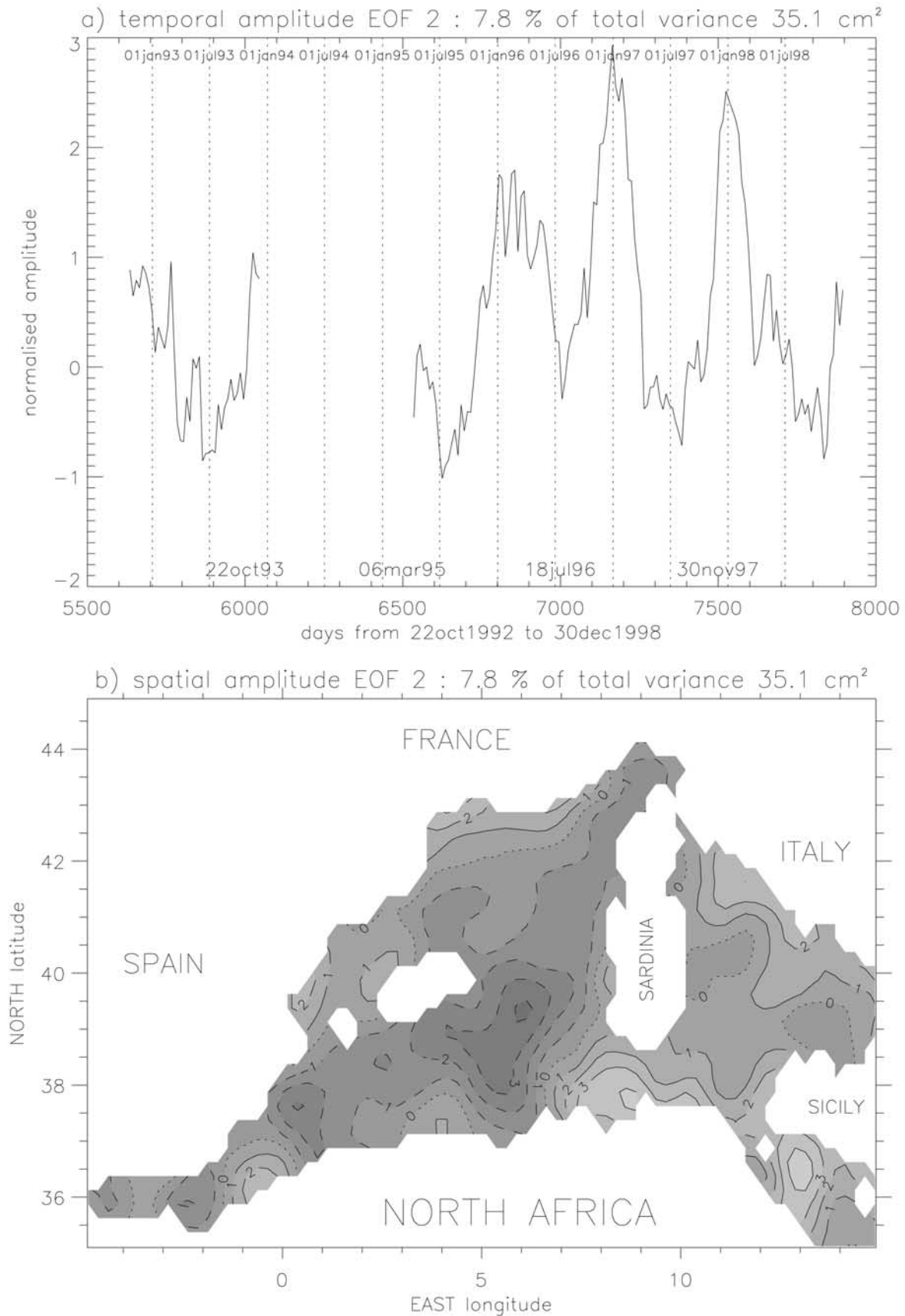


Figure 16. (a) Temporal normalized amplitude and (b) spatial amplitude with a contour interval of 1 cm for EOF 2 from SLA-SDA. Dashed, dotted and solid lines correspond to negative, null and positive values, respectively.

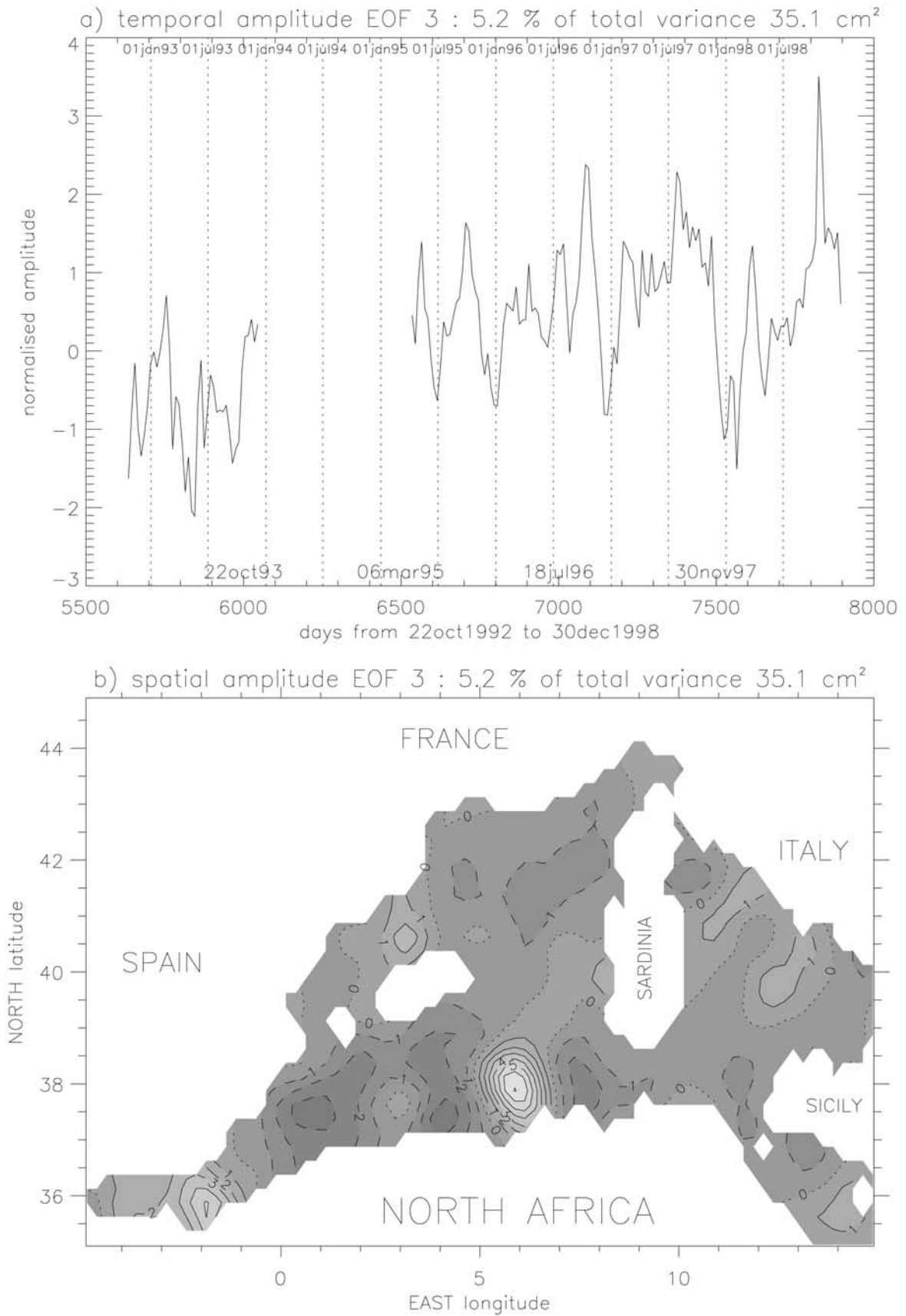


Figure 17. (a) Temporal normalized amplitude and (b) spatial amplitude with a contour interval of 1 cm for EOF 3 from SLA-SDA. Dashed, dotted and solid lines correspond to negative, null and positive values, respectively.

eastern part of the Alboran basin, but not along the Algerian coast. Therefore, the exact role of wind-forcing in the annual sea level variability remains uncertain.

5. Conclusions

[29] The aim of this study was to separate and evaluate the annual cycles of the western Mediterranean Sea level variability due to the steric effect and seasonal dynamic height variations. EOF analyses have been used to extract the annual variability in SLA and SST. The EOF results and the combination of SST and climatological hydrology allow an estimation of the steric effect, taking into account the temporal and spatial variations of the temperature in the mixed layer despite a few uncertainties on the mixed layer thickness, notably in the Alboran basin.

[30] This study shows that the time response of the steric effect is about 40 days and that the contribution of the intermediate and deep layers to the steric effect is not significant in general although it could be in some particular areas. The choice of the mixed layer thickness is, on the other hand, an important parameter affecting the estimation of the steric effect. A better knowledge of the mixed layer, whose temporal and spatial evolution depends mainly on sea surface fluxes and local turbulent mixing, is clearly necessary. Consequently, the use of the thermocline depth values from a mixed layer model [Caniaux *et al.*, 1998] should give more reliable estimations than the parameterisation used in this work.

[31] The highest amplitudes of the dynamic height annual variation and steric effect (>6 cm) are found in the Catalan and Tyrrhenian basins while the lowest amplitudes (<3 cm) are found on the path of the AW circulation, specially in the Channel of Sardinia and the Strait of Sicily where the mesoscale variability spreads the AW over the entire passage. As the annual temperature variations are smaller for the AW than for the older surface Mediterranean waters, the steric effect is expected to be weaker along the AW path. The annual cycles in the Alboran basin appear to be more complex than in the rest of the western Mediterranean Sea. The large annual sea level variation observed in that area is likely due to other forcing effects such as winds and AW inflow, inducing circulation variability, which could be only partially sampled by the MODB seasonal climatology.

[32] After removing the dynamic height annual variation and the steric effect in the mixed layer, the remaining annual sea level variability still represents about 50% of the residual sea level variability in the western Mediterranean Sea. The EOF analysis shows that one part of this signal is spatially homogeneous (3.5 cm) and can therefore be associated with the annual variation of water mass budget and some remaining annual steric and dynamic signal not correctly removed because of the too simple parameterisation of the mixed layer and because of lack of information in MODB seasonal climatology. The other part of the signal is mainly observed along the North African coast and could be associated with the annual variation of winds and fluxes at the Straits of Gibraltar and Sicily and their impact on mesoscale activity in the Alboran and Algerian basins. Also, the mean sea level used to get the SLA should be computed on a timescale longer than 3 years to avoid any local persistent anomalies due to long-lasting eddies.

[33] In summary, this study documents the relative importance of ocean dynamics and upper layer heat variability for the annual cycle of sea level in the western Mediterranean Sea. As one of the sea level component estimates and with the help of a mixed layer model and an improved climatology, it is shown that the annual amplitudes of the dynamic height and steric effect can be determined to an accuracy which makes it attractive for calibration and validation of the altimetric missions of Envisat and Jason. Both these missions have targeted calibration and validation sites in the northwestern Mediterranean Sea. Moreover, a better correction of the steric effect and atmospheric forcing in the altimetric measurement of sea surface height will be necessary for a precise estimation of the annual cycle of water mass budget, which is an important characteristic of the Mediterranean climatology.

[34] **Acknowledgments.** Catherine Bouzinac performed this scientific study in collaboration with Jordi Font and Johnny A. Johannessen during a research fellowship in the Earth Sciences Division of the European Space Agency Science and Technology Centre (ESTEC) in Noordwijk, Netherlands. During her visit, Johnny A. Johannessen was Head of the Ocean and Sea Ice Unit in the Earth Sciences Division.

References

- Alberola, C., C. Millot, and J. Font, On the seasonal and mesoscale variabilities of the northern current during the PRIMO-0 experiment in the western Mediterranean sea, *Oceanol. Acta*, 18(2), 163–192, 1995.
- AVISO, AVISO User Handbook: Merged TOPEX/POSEIDON Products, Ed. 3.0, *AVI-NT-02-101-CN*, Centre National d'Etudes Spatiales, Toulouse, France, July 1996.
- Ayoub, N., P.-Y. Le Traon, and P. De Mey, A description of the Mediterranean surface variable circulation from combined ERS-1 and TOPEX/POSEIDON altimetric data, *J. Mar. Syst.*, 18, 3–40, 1998.
- Benzohra, M., and C. Millot, Hydrodynamics of an open Algerian eddy, *Deep Sea Res.*, 42, 1831–1847, 1995.
- Bethoux, J.-P., Mean water fluxes across sections in the Mediterranean sea, evaluated on the basis of water and salt budgets and of observed salinities, *Oceanol. Acta*, 3(1), 79–88, 1980.
- Boukthir, M., and B. Barnier, Contribution of the observation from space to improve the knowledge of the fresh water budget of the Mediterranean Sea, in Satellite-based observation: A tool for the study of the Mediterranean basin, report, Cent. Natl. d'Etudes Spatiales, Tunis, 1998.
- Bouzinac, C., Variabilité spatiale et temporelle de la circulation superficielle dans la région du courant Algerien, Ph.D. dissertation, 125 pp., Univ. Pierre et Marie Curie, Paris, 1997.
- Bouzinac, C., J. Vazquez, and J. Font, CEOF analysis of ERS-1 and TOPEX/POSEIDON combined altimetric data in the region of the Algerian current, *J. Geophys. Res.*, 103, 8059–8071, 1998.
- Bouzinac, C., J. Font, and C. Millot, Hydrology and currents observed in the channel of Sardinia during the PRIMO-1 experiment from November 1993 to October 1994, *J. Mar. Syst.*, 20, 333–355, 1999.
- Brasseur, P., The Mediterranean Oceanic Data Base: A MAST initiative for ocean data and information management in the Mediterranean sea, *MTP News Lett.*, 2, 16–18, 1995.
- Caniaux, G., P. Andrich, H. Dolou, X. Durrieu du Madron, L. Izart, and G. Montesquieu, Un modèle opérationnel de prévision de couche mélangée océanique en Méditerranée occidentale, in *Satellite-based observation, a tool for the study of the Mediterranean basin*, report, Cent. Natl. d'Etudes Spatiales, Tunis, 1998.
- Cazenave, A., F. Mercier, M. C. Gennero, and P. Bonnefond, Present-day sea level changes in the Mediterranean and Black Seas from satellite altimetry, in *Proceedings of the 9th General WEGENER Assembly*, Statens Kartverk, Krokkeiva, Norway, 1998.
- Centre ERS d'Archivage et de Traitement, User Manual: ERS-1/2 products, report, Plouzane, France, 1996.
- Centre National d'Etudes Spatiales/NASA, JASON CALVAL plan, *CNES Rep. TP2-J0-PL-974-CN*, Cent. Natl. d'Etudes Spatiales, Toulouse, France, July 2000.
- Crepon, M., L. Wald, and J. M. Monget, Low-frequency waves in the Ligurian sea during December 1977, *J. Phys. Oceanogr.*, 87, 595–600, 1982.
- European Space Agency, Envisat Mission: Opportunities for science and applications, report, 67 pp., ESA Publ. Div., Eur. Space Res. and Technol. Cent., Noordwijk, Netherlands, 1998.

- European Space Agency, Envisat, the altimetry report: Science and applications, ESA Publ. Div., Eur. Space Res. and Technol. Cent., Noordwijk, Netherlands, 1999.
- Fofonoff, N. P., and R. C. Millard, Algorithms for compilation of fundamental properties of seawater, report, 53 pp., U. N. Educ. Sci. and Cult. Org., Paris, 1983.
- Font, J., J. Salat, and J. Tintore, Permanent features of the circulation in the Catalan sea, *Oceanol. Acta*, 9, 51–57, 1988.
- Font, J., C. Millot, J.-J. Salas, A. Julia, and O. Chic, The drift of modified Atlantic water from the Alboran sea to the eastern Mediterranean, *Sci. Mar.*, 62(3), 211–216, 1998.
- Fuda, J.-L., C. Millot, I. Taupier-Letage, U. Send, and J. M. Bocognano, XBT monitoring of a meridional section across the western Mediterranean sea, *Deep Sea Res.*, 1, 47, 2191–2218, 2000.
- Garcia, E., and J. Vazquez, Ocean-atmosphere coupling in the Mediterranean Sea from TOPEX/POSEIDON, ERS1 and AVHRR data, *Int. J. Remote Sens.*, 20(11), 2127–2147, 1999.
- Gascard, J.-C., Mediterranean deep water formation, baroclinic instability and oceanic eddies, *Oceanol. Acta*, 1, 315–330, 1978.
- Harzallah, A., D. L. Cadet, and M. Crepon, Possible forcing effects of net evaporation, atmospheric pressure and transients on water transports in the Mediterranean Sea, *J. Geophys. Res.*, 98, 12,341–12,350, 1993.
- Larnicol, G., P.-Y. Le Traon, N. Ayoub, and P. De Mey, Sea level variability in the Mediterranean Sea from two years of Topex/Poseidon data, *J. Geophys. Res.*, 100, 25,163–25,177, 1995.
- Le Traon, P.-Y., and P. Gauzelin, Response of the Mediterranean mean sea level to atmospheric pressure forcing, *J. Geophys. Res.*, 102, 973–984, 1997.
- Le Traon, P.-Y., and F. Ogor, ERS-1/2 orbit improvement using TOPEX/POSEIDON: The 2-cm challenge, *J. Geophys. Res.*, 103, 8045–8057, 1998.
- Le Traon, P.-Y., F. Nadal, and N. Ducet, An improved mapping method of multisatellite altimeter data, *J. Atmos. Oceanic Technol.*, 15(2), 522–534, 1998.
- Levitus, S., R. Burgett, and T. P. Boyer, World Ocean Atlas 1994, vol. 3 and 4, 99 pp., Natl. Ocean and Atmos. Admin., Silver Spring, Md., 1994.
- Madec, G., M. Chartier, P. Delecluse, and M. Crepon, A three-dimensional numerical study of deep water formation in the northwestern Mediterranean sea, *J. Phys. Oceanogr.*, 21, 1349–1371, 1991.
- Millero, F. J., and A. Poisson, International one-atmosphere equation of state for seawater, *Deep Sea Res., Part A*, 28, 625–629, 1981.
- Millot, C., Some features of the Algerian current, *J. Geophys. Res.*, 90, 7169–7176, 1985.
- Millot, C., Circulation in the Western Mediterranean Sea, *Oceanol. Acta*, 10(2), 143–149, 1987.
- Millot, C., Circulation in the Western Mediterranean Sea, *J. Mar. Syst.*, 20, 423–442, 1999.
- Pinot, J. M., and A. Ganachaud, The role of winter intermediate waters in the spring-summer circulation of the Balearic sea, *J. Geophys. Res.*, 104, 29,843–29,864, 1999.
- Press, W. H., S. A. Teukolsky, W. T. Vetterling, and B. P. Flannery, *Numerical Recipes: The Art of Scientific Computing*, 994 pp., Cambridge Univ. Press, New York, 1992.
- Robinson, I. S., *Satellite Oceanography*, 455 pp., John Wiley, New York, 1985.
- Taupier-Letage, I., and C. Millot, Surface circulation in the Algerian Basin during 1984, *Oceanol. Acta*, 9, 119–131, 1988.
- Tintore, J., P. La Violette, I. Blade, and A. Cruzado, A study of an intense density front in the eastern Alboran sea: The Almeria-Oran front, *J. Phys. Oceanogr.*, 18(10), 1384–1397, 1988.
- Vazquez, J., J. Font, and J.-J. Martinez-Benjamin, Observations on the circulation in the Alboran sea using ERS-1 altimetry and sea surface temperature data, *J. Phys. Oceanogr.*, 26, 1426–1439, 1996.
- Vazquez, J., K. Perry, and K. Kilpatrick, Sea surface temperature data set: User's reference manual, version 4.0, *JPL Publ.*, D-14070, April 1998.
- Vignudelli, S., P. Cipollini, M. Astraldi, G. P. Gasparini, and G. Manzella, Integrated use of altimeter and in situ data for understanding the water exchange between the Tyrrhenian and Ligurian seas, *J. Geophys. Res.*, 105, 19,649–19,663, 2000.
- Werner, F. E., A. Cantos, and G. Parilla, A sensitivity study of reduced-gravity channel flows with application to the Alboran Sea, *J. Phys. Oceanogr.*, 18, 373–383, 1988.
- Zlotnicki, V., L.-L. Fu, and W. Patzert, Seasonal variability in global sea level observed with Geosat altimetry, *J. Geophys. Res.*, 94, 17,959–17,969, 1989.

C. Bouzinac, European Space Research and Technology Centre, European Space Agency, Postbus 299, NL-2200-AG Noordwijk, ZH, Netherlands. (catherine.bouzinac@esa.int)

J. Font, Institut de Ciències del Mar CSIC, Passeig Marítim, 37–49, E-08003 Barcelona, Spain. (jfont@icm.csic.es)

J. Johannessen, Nansen Environmental and Remote Sensing Center, Edvard Griegsvei 3a, 5059 Bergen, Norway. (johnny.johannessen@nersc.no)